OKU Fen Bilimleri Enstitüsü Dergisi
7(2): 543-562, 2024

OKU Journal of The Institute of Science and Technology,
7(2): 543-562, 2024

Osmaniye Korkut Ata Üniversitesi Fen Bilimleri Enstitüsü Dergisi

Osmaniye Korkut Ata University Journal of The Institute of Science and Technology

Spark Plazma Sinterlenmiş Cu-SiC Kompozitlerinin Fiziko-Mekanik ve Elektriksel Özelliklerinin Değerlendirilmesi

Gökhan AÇIKBAŞ[1,2*], Nurcan ÇALIŞ AÇIKBAŞ[3]

[1] Mersin University, Department of Nanotechnology and Advanced Materials, 33110, Mersin, Türkiye
[2,3] Mersin University, Department of Metallurgical and Materials Engineering, 33110 Mersin, Türkiye

[1,2] https://orcid.org 0000-0002-5695-3658
[3] https://orcid.org 0000-0001-6193-8252
*Sorumlu yazar: gokhanacikbas@mersin.edu.tr

Araştırma Makalesi

Makale Tarihçesi:
Geliş tarihi: 21.06.2023
Kabul tarihi:22.10.2023
Online Yayınlanma: 11.03.2024

Anahtar Kelimeler:
Cu-SiC kompozitler
Kıvılcım plazma sinterleme
Sertlik
Mikroyapı
Elektriksel iletkenlik

ÖZ

Yapılan çalışmada, SiC takviyeli Cu matrisli kompozitler, hızlı yoğunlaşma sağlamak, zayıf ara yüzey bağını ve tane büyümesini ve fazlar arası bölgede istenmeyen fazları önlemek amacıyla kıvılcım plazma sinterleme tekniği ile üretilmiştir. Ayrıca takviye oranının (hacimce %10, 20, 30) ve partikül boyutlarının (1, 11, 24 µm) bakır kompozit malzemelerin fiziko-mekanik (yoğunluk, sertlik) ve elektriksel özelliklerine etkisinin belirlenmesi amaçlanmıştır. Kompozitlerin bulk yoğunluk değerleri Arşimet yöntemi, mikroyapı analizleri taramalı elektron mikroskobu (SEM) ve faz analizi X-Işınları difraksiyonu (XRD) tekniği ile belirlenmiştir. Uygun sinterleme rejiminin seçimi, kompozit numunelerin istenmeyen fazlar oluşmadan, Cu ve SiC tanecikleri arasında uygun ara yüzey bağı ile neredeyse tam yoğunluğa sahip Cu-SiC kompozitlerine ulaşılması için çok önemli olup bu çalışmada çok yüksek bulk yoğunluk (min. %99,48), düşük toplam gözeneklilik %0,15-0,52, iyi sertlik (HV 122-186) ve elektriksel iletkenlik elde edilmesini sağlamıştır. İnce SiC partikülleri (~1 mikron) kullanıldığında ve SiC miktarı arttığında, elektrik iletkenliğinde fazla bir kayıp olmadan kompozitlerin sertlik değeri etkili bir şekilde artmıştır. Bu bağlamda, yapılan çalışma, mükemmel sinerjik performansa sahip Cu-SiC kompozitlerinin üretimi için etkili bir çözüm sunmaktadır.

Evaluation of the Physico-Mechanical and Electrical Properties of Spark Plasma Sintered Cu-SiC Composites

Research Article

Article History:
Received: 21.06.2023
Accepted: 22.10.2023
Published online:11. 03.2024

Keywords:
Cu-SiC composites
Spark plasma sintering
Hardness
Microstructure
Electrical conductivity

ABSTRACT

In this study, SiC reinforced Cu matrix composites were produced by spark plasma sintering to provide rapid consolidation and to prevent weak interfacial bonding and grain growth, undesired phases at the interphase region. In addition, the influence of the reinforcement ratio (vol.% 10, 20, 30) and particle sizes (1, 11, 24 µm) on the physico-mechanical (density, hardness) and electrical characteristics of copper based composite materials was aimed. The bulk density values were determined by Archimedes' method, SEM, EDS, and XRD analysis were used to identify microstructural factors and phase analysis. It was found that the selection of the appropriate sintering regime is very important for composite samples to reach nearly fully dense Cu-SiC composites with proper interfacial bonding between Cu and SiC grains without the formation of any undesired phases, results in very high relative density (min. 99.48%), low total porosity (0.15-0.52), good hardness (HV 122-186) and electrical conductivity. When fine SiC particles (~1 micron) are

used and the amount of SiC increases, the hardness value of the composites was effectively improved without much loss in electrical conductivity. In this respect, this study provides an effective solution for the production of Cu-SiC composites with excellent combined performance.

To Cite: Açıkbaş G., Çalış Açıkbaş N. Evaluation of the Physico-Mechanical and Electrical Properties of Spark Plasma Sintered Cu-SiC Composite. Osmaniye Korkut Ata Üniversitesi Fen Bilimleri Enstitüsü Dergisi 2024; 7(2): 543-562.

1. Introduction

Due to its good ductility, corrosion resistance, high electrical and thermal conductivity, copper is one of the most widely used functional and structural engineering material (Abedi et al., 2021). However, its low hardness and yield strength, weak thermo-mechanical properties limit the use of pure copper in engineering applications. To overcome these limitations, copper matrix is reinforced with strong ceramic particles (Celebi et al. 2011; Dash et al. 2012; Thankachan et al., 2019; Torabi and Arghavanian, 2019; Shu et al. 2022). Silicon carbide (SiC) is the most common one as ceramic particulate reinforcement in many composite matrixes (Nair et al. 1985; Zhou and Xu, 1997; Mallik, et al. 2011; Mallik, et al. 2012; Suryanarayanan et al. 2013).

SiC improves the thermo-mechanical properties of copper at high temperatures due to its high hardness, strength, superior wear resistance, high decomposition temperature, high elastic modulus, excellent resistance to arc erosion and high thermal conductivity. Besides its excellent thermo-mechanical properties, SiC has good electrical conductivity (semiconductor material) and is used in many functional applications. SiC particulate-reinforced copper metal matrix composites are quite popular in electrical and electronic industries (e.g. electrical contacts, high performance switches, heat sinks, electronic packaging, resistance welding electrodes) because of their excellent thermo-mechanical and electrical conductivity properties as well as welding and brazing properties (Tjong and Lau, 2000; Shu and Tu, 2003; Brendel et al. 2004; Schubert et al. 2007; Efe et al. 2011; Efe et al. 2012; Shabani et al. 2014; Shabani et al. 2016; Moustafa and Taha, 2021). However, poor bonding between the copper matrix and SiC particles limits the properties of SiC reinforced copper matrix composites (Pelleg, et al. 1996).

Powder metallurgy (PM) and casting methods are common methods for the production of SiC reinforced Cu matrix composites (Tjong and Lau, 2000; Shu and Tu, 2003; Moustafa and Taha, 2021). PM method is generally preferred to casting. One of the most important stages in the production of SiC reinforced Cu matrix composites by powder metallurgy is the sintering process. The sintering technique creates significant changes, especially in the microstructure and thus in the material properties (Chmielewski et al. 2017).

Cu-SiC composites are sintered with conventional sintering, hot pressing (HP), hot isostatic pressing (HIP) and spark plasma sintering (SPS) (Kuskov et al. 2021; Abedi et al. 2022). The main problem in the production of SiC reinforced copper matrix composites with sintering is the differences in melting/decomposition temperatures of Cu and SiC (T_mCu: 1085 ^oC and T_dSiC: 2830 ^oC). At high

temperatures during sintering, silicon and carbon dissolve in the copper matrix (Sundberg, et al. 2005). With the dissolution of silicon in copper, new Cu-Si phases are formed, and these phases adversely affect the thermal, mechanical and electrical properties of MMCs. The affinity of carbon dissolved from SiC to Cu and the solubility of this carbon in Cu are negligible (Schubert, et al. 2007). In addition, carbon dissolved from SiC forms an interlayer at the metal-ceramic interface that prevents good interfacial bonding (Grzonka et al. 2015; Nosewicz et al. 2019). On account of this, rapid consolidation is required for the production of Cu-SiC composites to prevent these negative effects. Among other sintering techniques, spark plasma sintering (SPS) provides better densification with high heating and cooling rates and short dwell time (Hu et al. 2020; Abedi et al. 2022). During SPS, the mass transfer rate increases by evaporation and convection at the point of contact between the particles thanks to the electric current, and at the same time, oxides are removed from the surface of the copper particles with the increase in temperature. The activation energy required for diffusion is reduced, which increases the rate of material densification.

In literature there are some studies on the production of Cu-SiC composites with SPS (Zhang et al. 2003; Akbarpour and Alipour, 2017; Chmielewski et al. 2017; Mallikarjuna et al. 2017; Bazarnik et al. 2019; Chmielewski et al. 2019; Nosewicz et al. 2019; Hu et al. 2020). In these studies, it is stated that SPS provides a better densification rate. However, even if Cu-SiC composites are produced with SPS, it has been reported that the short heating time at maximum temperature does not protect the surface of silicon carbide from negative interactions with the copper matrix (Nosewicz et al. 2019). It should be noted that with the selection of the appropriate sintering regime and the appropriate production process, the mentioned negative situations can be prevented (Abedi et al. 2022). Thus, composites with good Cu-SiC interface can be developed without the need for extra processing stages (e.g. coating of SiC particles). Therefore, in this study, SPS sintering temperature was chosen as 800^{o}C using thermodynamic data (Zhang et al. 2003). Cu-SiC composites were produced with different SiC particle sizes and ratios, and microstructure-property relations were investigated and interface interactions of SiC-Cu phases were studied with special attention.

2. Materials and Methods

2.1. Materials

In this study, Cu powder with >99.9 % purity and an average particle size of ~20 μm (Sentesbir, İzmir, Turkey) was used as matrix material in the production of metal matrix composites. Three different SiC powders with high purity (99.99 %) and average particle size of 1 (coded as SC-1), 11 (coded as SC-11) and 24 (coded as SC-24) micrometers were used as reinforcement material (Saint Gobain, France).

2.2. Composite Production Process and Characterization

Cu and SiC powders are weighed in accordance with the recipes given in Table 1, and mixed in a Fritsch Pulverisette Planetary Mill for 10 minutes at 200 rpm, adjusting the ball and powder volume to

be 1: 1 has been kept. In order to prevent oxidation on the surface of the powders, a composite mixture was prepared by using a short mixing time, a low mixing speed and isopropyl alcohol was used instead of water. The composite mixtures were dried in an oven at 105 °C. The dried powders were kept at room temperature in a desiccator in vacuum bags until sintering.

Table 1. Cu-SiC composite compositions

Sample Codes	SiC (vol. %)	SiC Particle Size, µm	Copper (Cu) (vol. %)
Cu	0	-	100
A1	10	1	90
A2	20	1	80
A3	30	1	70
B1	10	11	90
B2	20	11	80
B3	30	11	70
C1	10	24	90
C2	20	24	80
C3	30	24	70

Composite powder mixtures were sintered by spark plasma sintering method (SPS, HPD-50, FCT System GmbH, Germany) in a vacuum atmosphere at uniaxial pressure of 50 MPa, at a heating rate of 100^{o}C/min., at 800 ^{o}C for 10 minutes, and pellets with a diameter of ~20 mm and a thickness of ~1.5 mm were obtained. Phase analyzes of the starting samples and sintered composite samples were performed using X-ray diffraction (XRD, Rigaku-SmartLab) device at a rate of 2 ^{o}/min between the 30-80^{o}, 2 thetas. The particle shape and size of the starting powders and the microstructures of the sintered composite structures were investigated using FEI, Quanta 650 Field Emission model scanning electron microscope (FEG-SEM) with back scattered electron (BSE) detector and energy dispersive X-ray spectroscopy (EDS). Theoretical density values of the composite samples were calculated according to the mixing rule. The bulk density values of the composites were calculated using the Archimedes principle (Açıkbaş, et al. 2018; Açıkbaş, 2018). % Theoretical density values of composites were calculated by dividing the bulk density to theoretical density of composites (Açıkbaş, 2018). The hardness of the composite samples was determined under 300 g load by taking 5 measurements from each sample and using the Emcotest DuroScan 20 model Vicker's Microhardness device. The electrical conductivities of samples were measured by eddy currents as %IACS (Fischer, Sigmascope SMP350). A composite production flow chart and characterization scheme are given in Fig. 1.

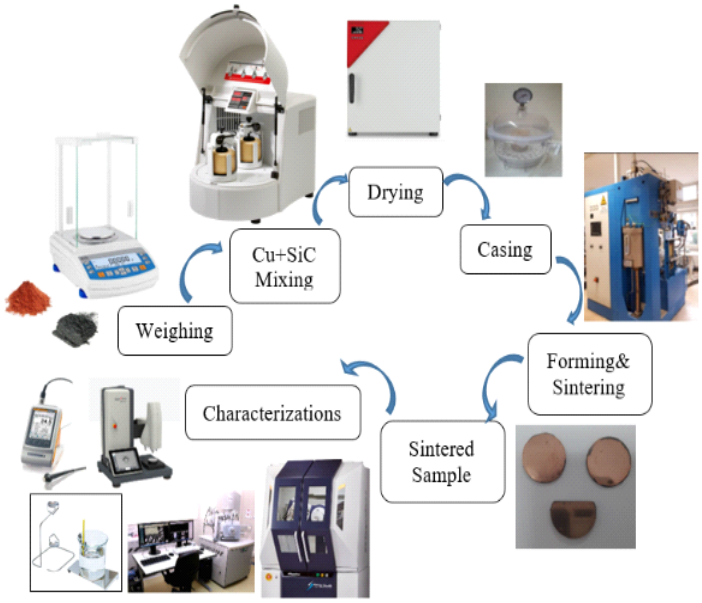

Figure 1. Composite production flow chart and characterization scheme

3. Results and Discussion

3.1. Characterization of Starting Powders

Since the chemistry (content) and physical properties of the starting powders used in the experimental studies affect the material properties and performance, the characterization of the starting powders was carried out first. The XRD analysis of the SiC powders showed that α-SiC as a major phase in the form of 6H, 4H and 15 R polytypes in all samples (Fig. 2.). Each symbol in the SiC structures has a distinct meaning. Both 4H SiC and 6H-SiC represent the hexagonal crystal system, and the difference between them lies in their stacking sequences. In 4H SiC, the layers are stacked in an ABCB array while in 6H-SiC the stacking array is ABABAB. R denotes the family of rhombohedral polytypes, for example, 15R-SiC. Representative SEM images of initial SiC powders with different particle sizes are given in Fig. 3. As seen from the images, SC-1 powder is very fine and average particle size around 1 µm. On the other hand, SC-11 and SC-24 powders are coarse, and the average particle sizes ~11 and 24 µm, respectively. The SiC particle shapes are irregular and have sharp edges. Figure 4 a,b revealed particle size distribution graphs of SC-11 and SC-24 powders obtained by laser diffraction method. The results show that SC-11 powder has an average particle size of 11.47 µm (d_{50}) while SC-24 powder has an average particle size of 22.97 µm (d_{50}).

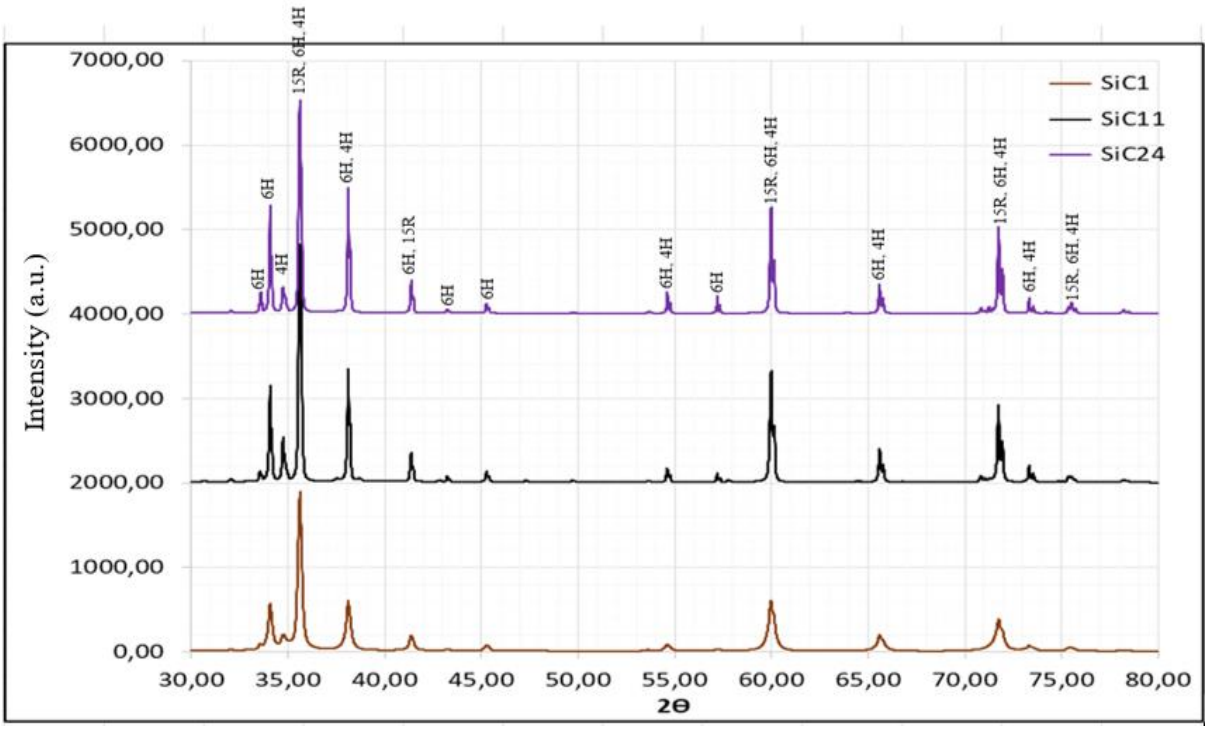

Figure 2. XRD graph of starting SiC powders: α-SiC as a major phase in the form of 6H, 4H and 15 R polytypes

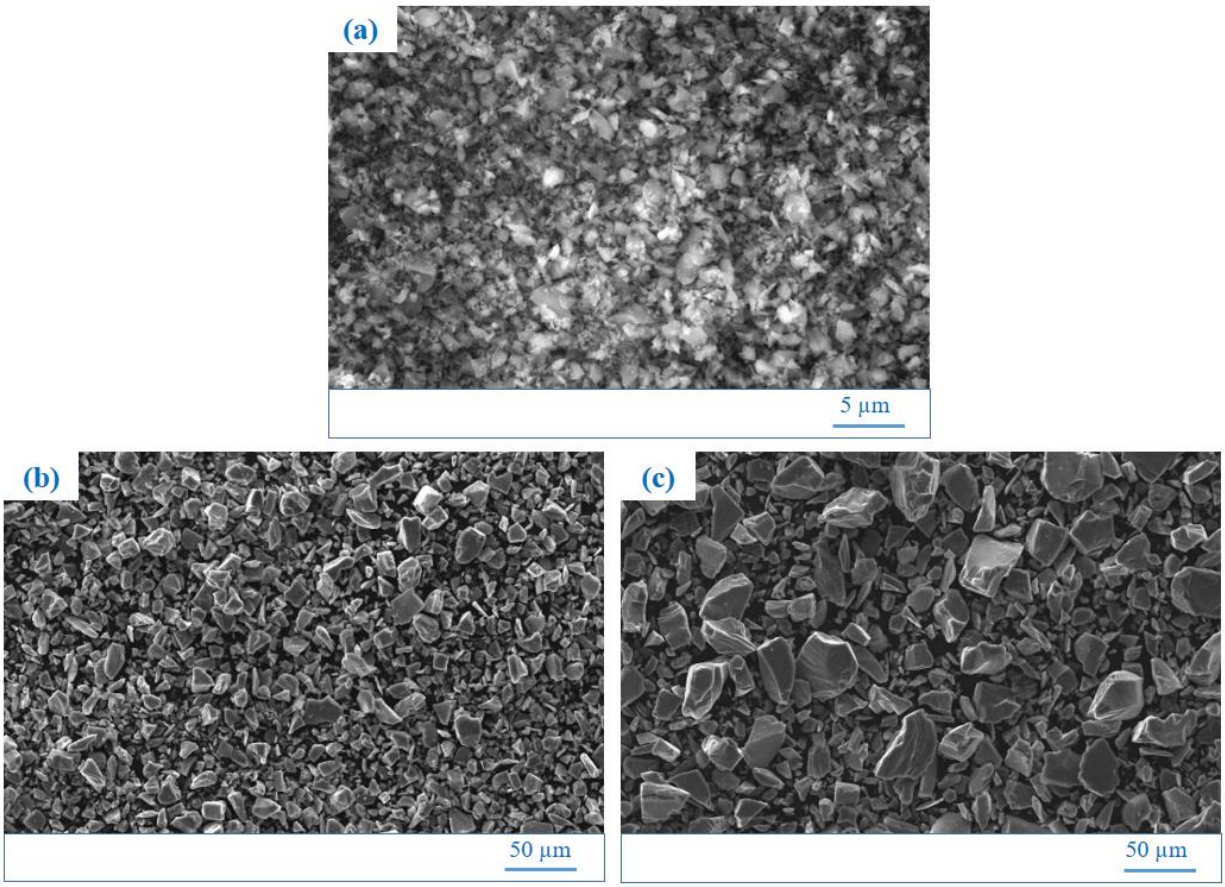

Figure 3. Representative SEM images of starting SiC powders with different particles sizes (a) SC-1 powder, (b) SC-11 powder, (c) SC-24 powder

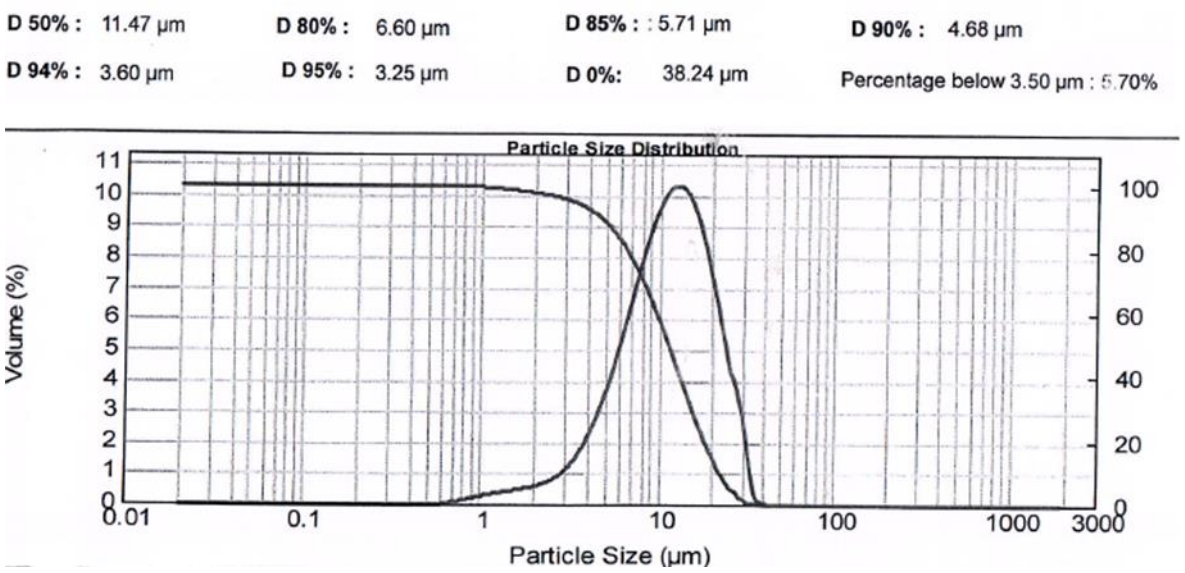

(a)

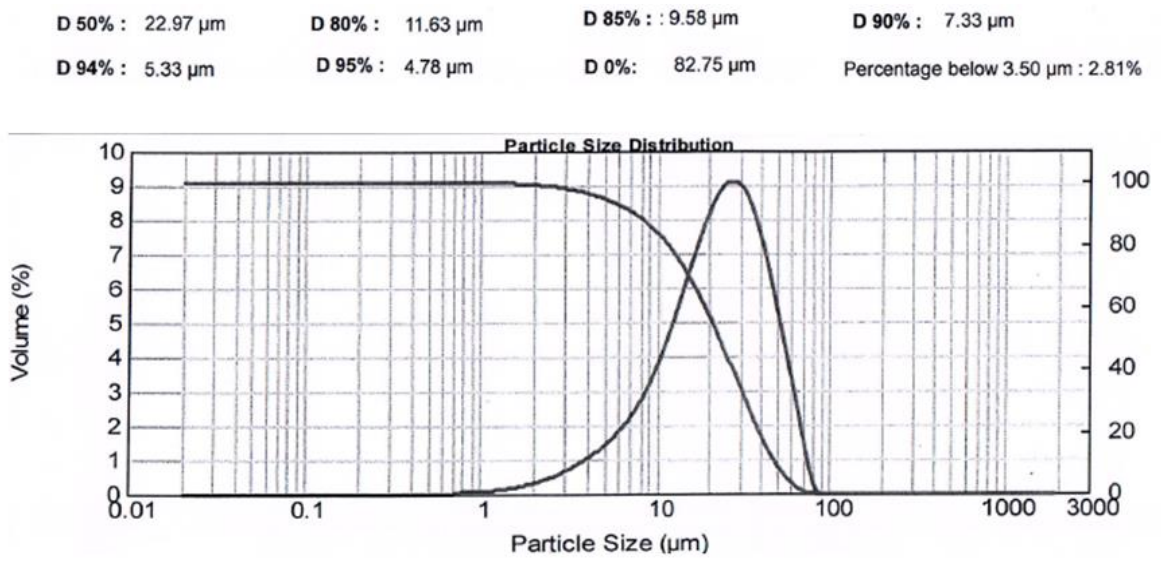

(b)

Figure 4. Particle size distribution graphs of (a) SC-11 and (b) SC-24 powders.

The XRD graph of initial Cu powder is given in Fig. 5. The copper powder is pure and just copper phase is available. All the copper particles almost spherical in shape, and diameters change between 5 microns and 60 microns (Fig. 6).

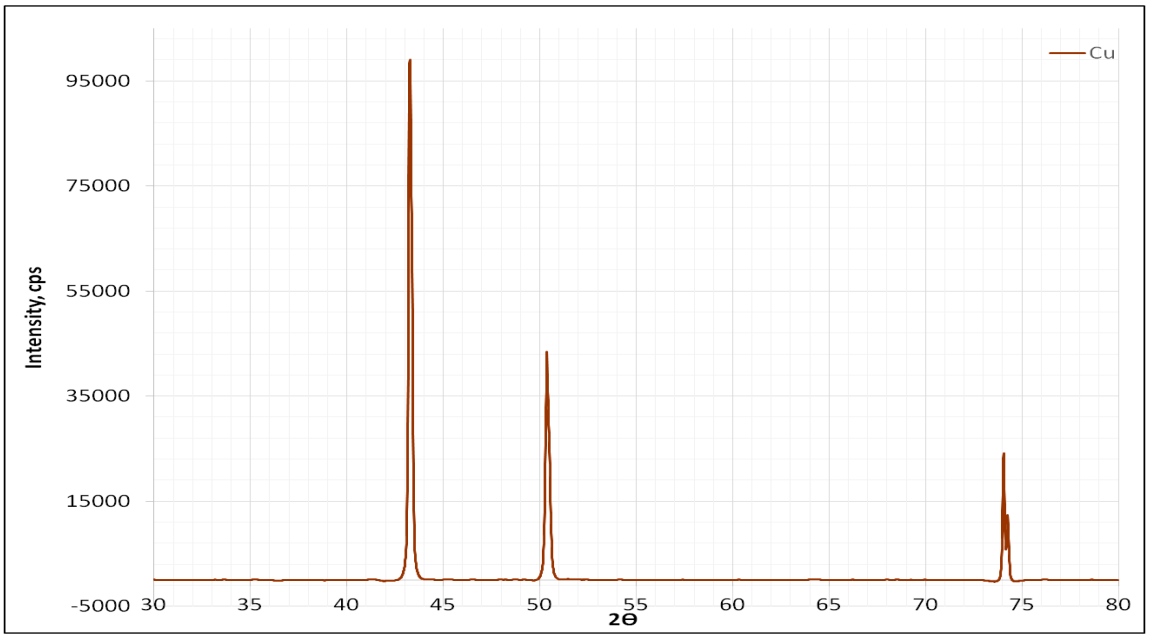

Figure 5. The XRD graph of initial Cu powder used as matrix in the composite production

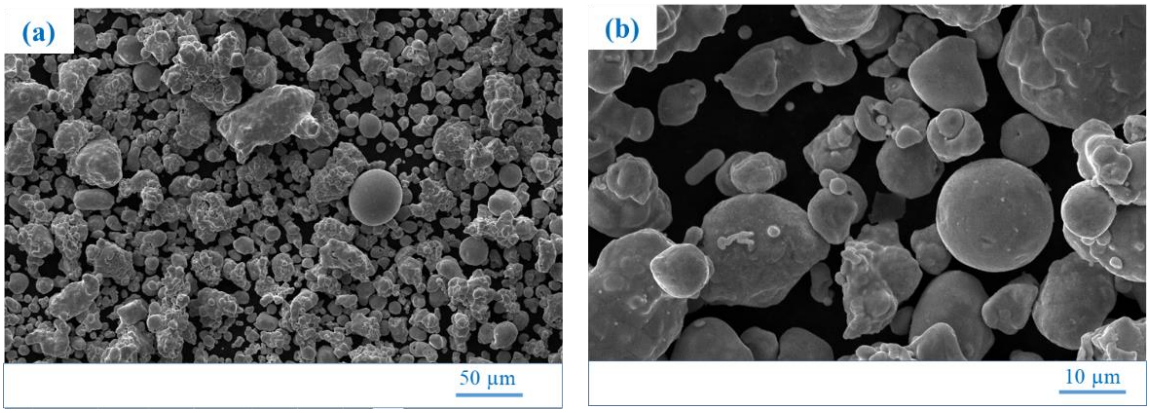

Figure 6. Representative SEM images of initial Cu powder

After the characterization studies on the initial powders, it was seen that Cu and SiC powders did not contain any impurities, Cu powders were approximately 20 µm in size and spherical shaped, SiC powders were 1, 11 and 24 µm average particle sizes and irregular shaped and has sharp corners.

3.2. Densification, Phase and Microstructural Characterization

The theoretical density of the produced composites was calculated for the assumed volume contents, using the density of silicon carbide ρ_{SiC} = 3.21 g/cm^3 and the density of copper ρ_{Cu}= 8.93 g/cm^3 were assumed from suppliers' specifications. The measured bulk density, theoretical density% values of Cu-SiC composites were given in Table 2. The spark plasma sintered Cu-SiC composites show superior densification behavior with high % theoretical density values (min 99.48 and max 99.85). These results approved that the applied sintering regime is appropriate for designed compositions. The use of a finer SiC particle size (1 µm) improved the densification of the composite material only to a

small extent. In all compositions, as the amount of SiC increased and the SiC particle size became coarser, the bulk density and relative density decreased, and the pore amount increased slightly. It was observed that in all examined cases, the composites were effectively sintered and well densified. The total porosity values are very low and change between 0.15% to 0.52%. Chmielewski et al. conducted study on Cu-SiC composites (SiC content vol.% 5-25, SiC particle size 80 μm, Cu powder particle size 40 μm) and they sintered samples with SPS (sintering temperature = 950 °C, heating rate = 100 °C/min, holding time = 10 min, and pressure = 50 MPa) and they found relative densities change between 98.4 to 99.1% (Chmielewski et al., 2017). The general trend is that the temperature increase causes the final density of the consolidated materials to increase. This phenomenon is valid until reaching relatively high final densities. The selection of the appropriate sintering regime is very important for composite samples to reach a high density. Compared to the study of Chmielewski et al., the use of finer Cu and SiC starting powders resulted in completely dense and desirable phase development at a lower temperature (150 degrees less). In our case, the 150°C increase in SPS temperature may have evaporated the Cu metallic phase and eventually caused a reduction in final density. The obtained density and porosity results showed that the applied sintering regime was very effective for the produced composites. A better densification of composites obtained with A1 sample which has low SiC content and fine SiC particle size (1 μm). As the amount of SiC and particle size increased, a slight decrease in the relative density and a slight increase in the amount of porosity were observed. Since the fine SiC powders are homogeneously dispersed in the copper matrix powders, there was no negative effect on the condensation behavior of the composite. This shows that the applied mixing procedure in the planetary mill is very effective.

Table 2. The bulk density, theoretical density, % theoretical density, % total porosity values of Cu-SiC composites with varying amount of SiC reinforcement and particle sizes, produced by SPS

Sample Code	**SiC particle sizes (μm)**	**SiC content (vol. %)**	**Theoretical Density** (g/cm^3)	**Bulk Density** (g/cm^3)	**%Theoretical Density**	**%Total Porosity**
A1	1	10	8.34	8.32±0.010	99.85	0.15±0.011
A2	1	20	7.76	7.74±0.012	99.74	0.26±0.012
A3	1	30	7.19	7.17±0.014	99.69	0.31±0.012
B1	11	10	8.34	8.31±0.011	99.71	0.29±0.013
B2	11	20	7.76	7.73±0.013	99.64	0.36±0.014
B3	11	30	7.19	7.16±0.016	99.56	0.44±0.014
C1	24	10	8.34	8.31±0.012	99.64	0.36±0.012
C2	24	20	7.76	7.73±0.014	99.58	0.42±0.013
C3	24	30	7.19	7.15±0.015	99.48	0.52±0.014

The microstructural images of Cu-SiC composites after sintering is given in Fig. 7. In the definition of SEM-BSE images, the dark area represents the SiC reinforcement phase, while the gray color represents the Cu matrix. There is almost no porosity in all composite microstructures. These observations coincided with the calculated density and porosity results. As can be seen from the SEM-BSE images, it was observed that the SiC ceramic phase was homogeneously dispersed in the Cu matrix, regardless of the volume fraction. The size and grain boundaries of Cu grains are evident in all A-coded samples and very similar in all SiC content, with a SiC grain size is very fine (1 μm). Cu grains are surrounded by SiC particles. The grain size of Cu grains are changes between 10-70 μm and these grains are relatively equiaxial. In the applied SPS regime, the sintering process of the SiC grains did not occur**.** The starting powders in SPS samples generally retain their initial dimensions. When the particle size of the starting SiC powder used became coarser (11 and 24 μm), the size of the Cu grains decreased. The microstructures of B and C coded composite samples with the SiC particle size is 11 and 24 μm are similar in terms of homogeneous distribution of SiC grains, Cu grains and porosity, as shown in Fig. 6. In the composites containing 20% and 30% SiC, the ceramic particles led to the thinning of the copper grains. As the amount of SiC increased, the aggregation of SiC grains increased. When fine SiC powder was used (1 μm), the aggregation of SiC grains increased as the amount of SiC increased. As SiC particle size increased at constant additive ratio, aggregation of SiC grains around copper grains decreased as expected (see Fig. 8). Since there is a copper phase between fine SiC grains, the aggregation of SiC grains did not adversely affect the densification behavior of the composite.

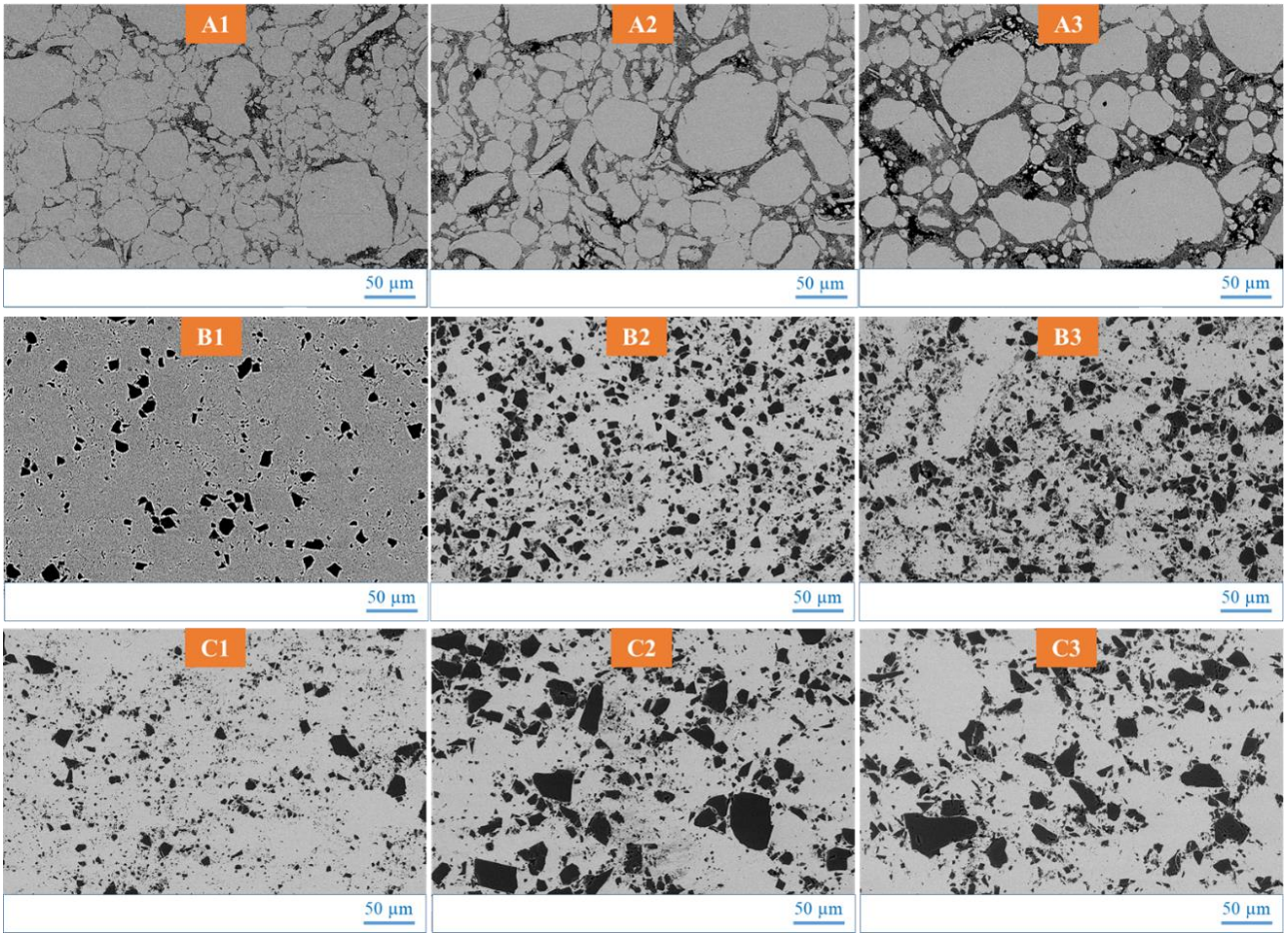

Figure 7. SEM-BSE images of the microstructures of Cu–SiC composites after SPS processing at low magnification (1000 x) with 10%, 20, 30 SiC content

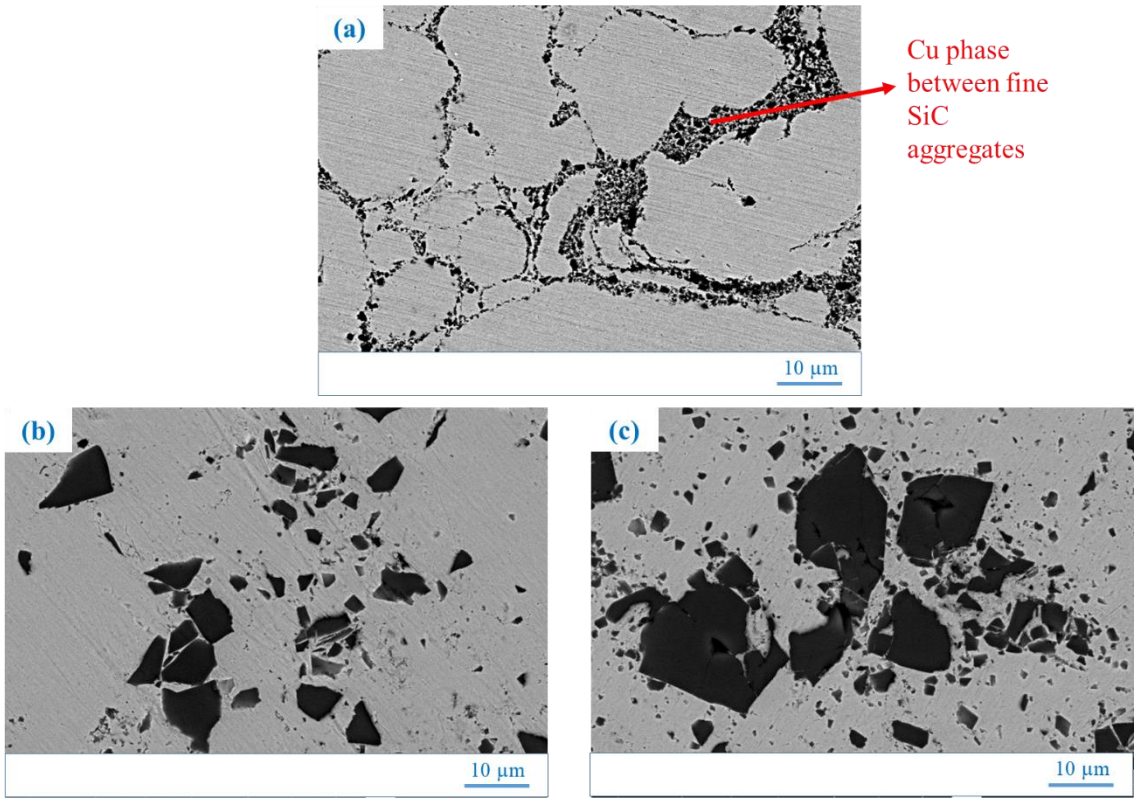

Figure 8. SEM-BSE images of the Cu–SiC composites with 10 vol.% SiC addition after SPS

The detailed SEM-BSE analysis of the matrix/reinforcement interface is given in Fig. 9. There are two broad ways to look at the interface's importance. First, the interface's physical condition and the presence of potential property-changing material flaws at or close to the interface. The chemical condition of the interface is the second consideration, as interactions between the metal matrix and ceramic reinforcements during processing could result in the formation of a new phase. SEM images show that there are no additional phases and defects (porosity, nanocracks, etc.) in the interfacial regions between Cu and SiC grains in all composites during the sintering process, regardless of SiC particle size and amount. The formation of Cu_3Si phase has been reported in the literature as one of the important problems affecting the performance of the material in the production of Cu-SiC composites (Schubert, et al. 2007; Balog, et al. 2010). Cu_3Si phase formation at the Cu matrix SiC phase interphase was not observed in this study. The obtained Cu matrix SiC reinforcement interface images show that the applied sintering regime and other process parameters are convenient and thus effective composite performance can be achieved by this way. From the SEM images at high magnifications, it is clear that no other phase formation takes place between the Cu matrix and the SiC reinforcement and there is a good bonding between Cu and SiC grains. The results of XRD and SEM-EDX analyzes also confirm this situation (see Fig. 10 and 11).

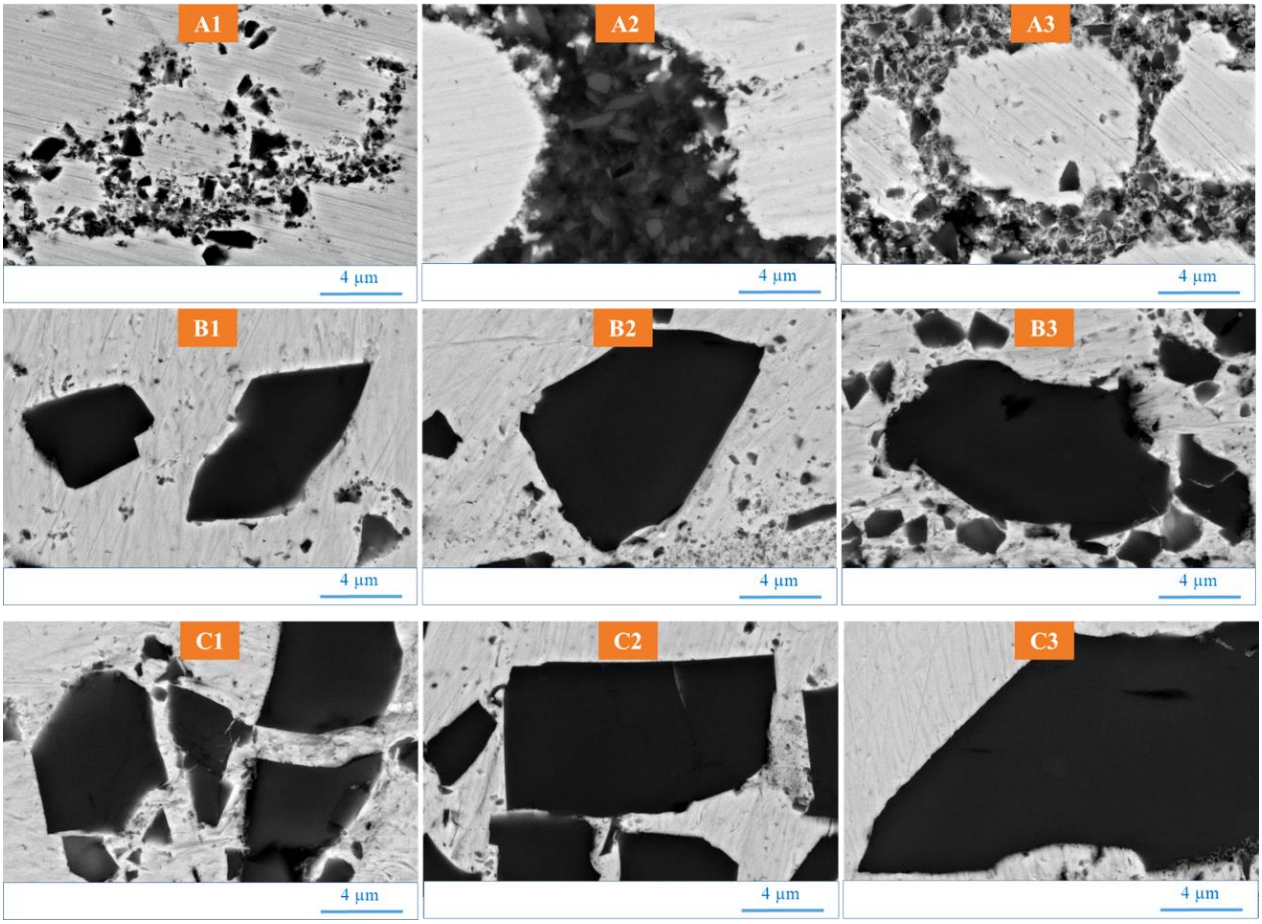

Figure 9. SEM-BSE images of Cu-SiC interface in composites with different SiC content and particle sizes

Additionally, the analytical investigation of elements was carried out by SEM-EDS line analysis. The existence and deploying of elements of the A2 and C2 coded samples are presented in Fig. 10. According to SEM-EDX line analyses at the interphase regions, Si and C elements did not react with the copper matrix. No oxygen was detected at the Cu-SiC interface in the C2 coded composite sample, while very little oxygen was detected in the A2 coded sample due to fine SiC particles. The similar observations were obtained in the study conducted by Celebi et all (Efe, et al. 2012).

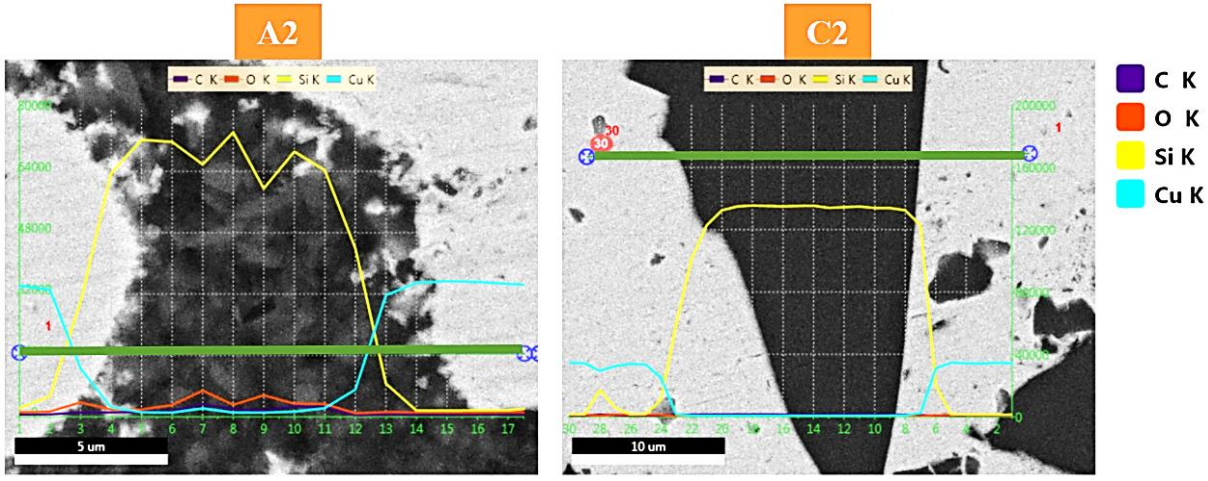

Figure 10. SEM/EDS line analysis of Si-C-Cu-O elements for Cu-SiC composites

The XRD patterns of the all sintered composite samples which have different amount of SiC content and particle sizes are given in Fig. 11. The XRD graphics showed that the all composite samples composed of copper and SiC phases. The formation of any undesirable interphases (Cu_3Si etc.) was not observed, and hence XRD analysis results coincided with the SEM-BSE and SEM-EDX analysis. As SiC content and SiC particle size increased, SiC peak intensity increased in the XRD plot of Cu-SiC composites. The absence of any phase other than Cu and SiC phases in Cu-SiC composites is very crucial in electrical conductivity as well as thermo-mechanical properties. As a summary, the contact zones between the Cu matrix and the SiC reinforcements following SPS show no signs of undesired phases, voids, de-bonding, or cracking.

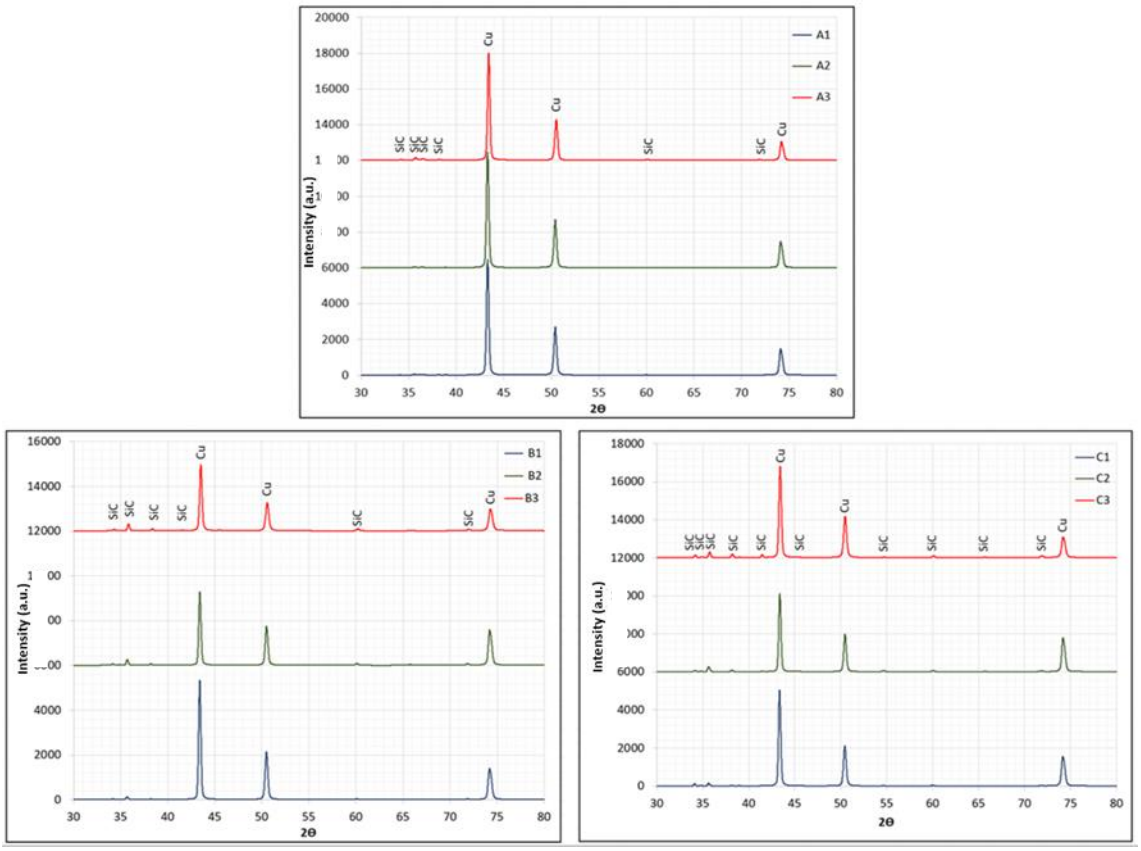

Figure 11. XRD patterns of spark plasma sintered Cu-SiC composites with different SiC content and particle sizes

3.3. Hardness

The use of a rigid ceramic second phases is a very effective method for improving the hardness of a metal matrix. The Vickers microhardness test results of spark plasma sintered Cu matrix composites with different SiC particle sizes and content were given in Fig. 12. It is found that the micro hardness of the pure Cu sample (coded SB) produced with SPS was 110, the hardness value improved significantly with the addition of SiC phase (between 122 and 186). The presence of hard SiC particles increases the hardness of the Cu matrix due to the Orowan strengthening mechanism. SiC

effectively prevents dislocation slippage and gliding, which boosts the overall strength of the metal matrix. On the other hand, when high volume fractions of fine SiC particles are added to the copper matrix, indent is more likely to come into hard SiC particles, resulting in higher hardness values. The second influence on increase in hardness could be dislocation density caused by thermal inconsistency between the Cu matrix and the ceramic reinforcement. These pressures create dislocations at the matrix particle interface, which can accumulate as reinforcement content increases. As well as, when SiC particles hindered grain growth in composite samples, the microstructure was homogenous in terms of grain size, and the hardness values were higher when compared to metal matrix.

When finer SiC grains were used and the amount of SiC increased, the hardness value of the composites increased. This result may be due to the effect of fine grain size (Hall-petch effect) (Abedi, et al. 2022). The results obtained are generally consistent with the behavior of fine-grained materials. With fine particles (small inter-particle spacing), constrained deformation of the ductile matrix limits plastic flow, thus contributing to the hardness and strength. The hard and tightly packed SiC particles, which are homogeneously dispersed around the copper grains, prevent the movement of dislocations.

On the other hand, one of the most important factors affecting hardness is relative density and therefore porosity. The applied sintering regime caused effective consolidation of the microstructure, and the densification behavior of all composites was very good. Since Cu-SiC composites have low porosity, their hardness values are high and close to each other.

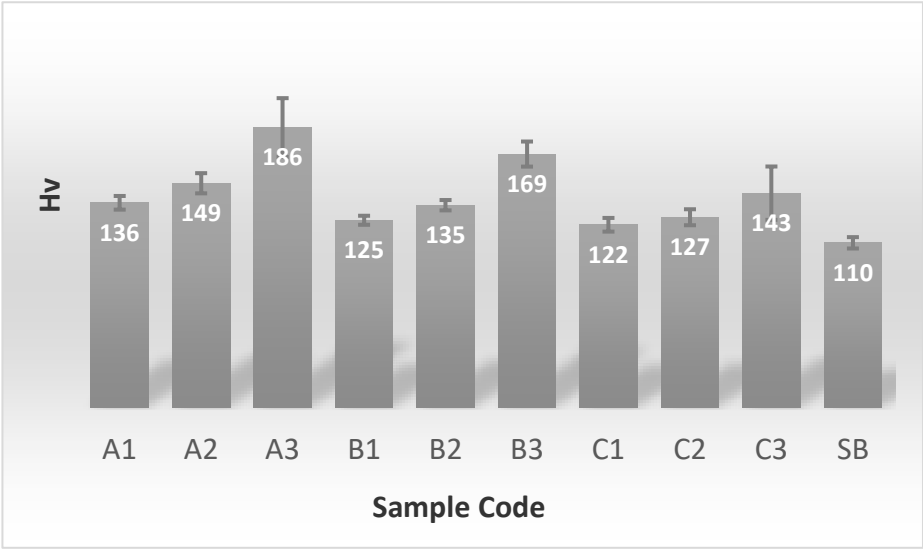

Figure 12. Microhardness test results of Cu-SiC composites

3.4. Electrical conductivity

Electrical conductivity of Cu-SiC composites are affected by electrical conductivity of the materials that make up the composites, microstructural parameters like grain size, shape, porosity, volume fractions and distributions of constituent phases (Moustafa, and Taha, 2021). Regardless of SiC particle size and amount, the relative density values of the produced composites are quite high and the

amount of pores is low. On the other hand, the absence of any phases except Cu and SiC and the strong interfacial bond between Cu-SiC grains affect the electrical conductivity positively. The electrical conductivity results of produced Cu-SiC composites were given in Fig. 13. As the amount of SiC increased in the Cu-SiC composites produced, the electrical conductivity of the composites decreased. SiC grains create a barrier for copper electrons that provide electrical conductivity and cause a decrease in electrical conductivity. The electrical conductivity values of Cu-SiC composites produced using coarse SiC particles are higher than those produced using fine SiC particles. This result is due to the fact that the fine SiC grains surround the Cu grains better and form a barrier. The results obtained are consistent with the studies in the literature (Efe, et al. 2012). As the SiC grain size increases, the SiC grains in the composite structure lose their coupling and act as isolated clusters in a highly conductive phase. In the study, the homogeneous distribution of SiC grains in the copper matrix and the absence of any interphase at the Cu-SiC grain interface and their good bonding ensured that the produced composites had good electrical conductivity. The electrical conductivity values in the 10% SiC added composites were around 66.4 in the fine SiC-grained composites, increased to 76.8 when the SiC grain size increased to 11 µm, and increased to 81.8 when the SiC grain size increased to 22 µm. Similar trend was observed in all SiC ratios.

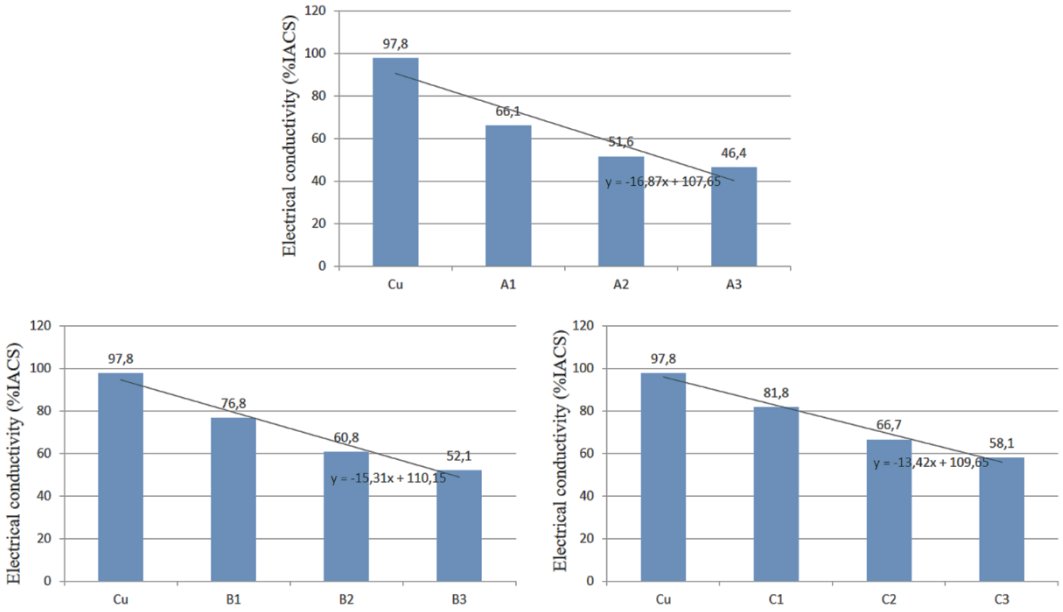

Figure 13. Electrical conductivity of spark plasma sintered Cu–SiC composites

4. Conclusions

In this study, SiC reinforced Cu matrix composites were manufactured using spark plasma sintering to offer quick consolidation while preventing weak interfacial bonding, abnormal grain growth and undesirable phases in the interphase region. Furthermore, the effect of the reinforcement ratio (vol.% 10, 20, 30) and particle sizes (1, 11, 24 µm) on the physico-mechanical (density, hardness) and electrical properties of copper composite materials was intended. Previously reported that, even if Cu-

SiC composites are produced with SPS, the short heating time at maximum temperature does not protect the surface of silicon carbide from negative interactions with the copper matrix and hence undesired phase evolution inevitable. In this conducted study, Cu-SiC composites sintered with SPS and sintering temperature was determined by using thermodynamic data, besides in order to prevent oxidation on the surface of the powders, a composite mixture was prepared by using a short mixing time, a low mixing speed and isopropyl alcohol was used instead of water.

The obtained experimental results revealed that, composites with good Cu-SiC interface bonding, very high relative density (min. 99.48%), low total porosity (0.15-0.52), good microhardness (HV 122-186) and electrical conductivity were developed without the need for extra processing stages (e.g. coating of SiC particles). Regardless of the volume fraction, SEM images demonstrated that the SiC ceramic phase was homogeneously dispersed in the Cu matrix. The hardness value of the composites was effectively improved without significant loss in electrical conductivity when fine SiC grains (1 μm) are utilized, and the amount of SiC is increased. The size of the Cu grains in composite microstructure decreased as the particle size of the starting SiC powder increased (11 and 24 μm). The Cu matrix SiC reinforcement interphase images produced suggest that the applied sintering regime and other process parameters are appropriate, and hence effective composite performance may be accomplished in this manner.

Conflicts of interest

There are no conflicts to declare.

Author contributions

Gökhan Açıkbaş: Conceptualization, Methodology, Validation, Visualization, Resources, Investigation, Interpretation of data, Revised it critically for important intellectual content, Writing - original draft and review; Nurcan Çalış Açıkbaş: Methodology, Validation, Interpretation of data, Revised it critically for important intellectual content, Writing-editing.

Acknowledgements

I would like to thank Erhan Ayas, a member of Eskişehir Technical University Advanced Technology Materials Laboratory, for his support in the production of composites with SPS.

References

Abedi M., Asadi A., Vorotilo S., Mukasyan AS. A critical review on spark plasma sintering of copper and its alloys. Journal of Materials Science 2021; 56: 19739–19766.

Abedi M., Sovizi S., Azarniya A., Giuntini D., Seraji ME., Hosseini HRM., Mukasyan A. An analytical review on spark plasma sintering of metals and alloys: From processing window,

phase transformation, and property perspective. Critical Reviews in Solid State and Materials Sciences 2022; 1-46.

Açıkbaş G., Özcan S., Çalış Açıkbaş N. Production and characterization of a hybrid polymer matrix composite. Polymer Composites 2018; 39(11): 4080-4093.

Açıkbaş G. Interfacial and physico-mechanical properties of walnut shell fiber reinforced polyester matrix composites. Materials Testing 2018; 60(5): 510-518.

Akbarpour MR., Alipour S. Wear and friction properties of spark plasma sintered SiC/Cu nanocomposites. Ceramics International 2017; 43(16): 13364-13370.

Balog M., Kováč J., Šatka A., Haško D., Zhang J., Crimp MA., Vávra I. SiC-based cermet with electrically conductive grain boundaries. Materials Characterization 2010; 61(4): 420-426.

Bazarnik P., Nosewicz S., Romelczyk-Baishya B., Chmielewski M., Nędza AS., Maj J., Langdon TG. Effect of spark plasma sintering and high-pressure torsion on the microstructural and mechanical properties of a Cu–SiC composite. Materials Science and Engineering: A 2019; 766: 138350.

Brendel A., Popescu C., Leyens C., Woltersdorf J., Pippel E., Bolt H. SiC-fibre reinforced copper as heat sink material for fusion applications. Journal of Nuclear Materials 2004; 329: 804-808.

Celebi Efe G. F., Altinsoy I., Ipek M., Zeytin S., Bindal C. Some properties of Cu-SiC composites produced by powder metallurgy method. Kovove Materialy 2011; 49: 131–136.

Chmielewski M., Pietrzak K., Strojny-Nedza A., Kaszyca K., Zybala R., Bazarnik P., Nosewicz S. Microstructure and thermal properties of Cu-SiC composite materials depending on the sintering technique. Science of Sintering 2017; 49(1).

Chmielewski M., Nosewicz S., Wyszkowska E., Kurpaska Ł., Strojny-Nędza A., Piątkowska A., Pietrzak K. Analysis of the micromechanical properties of copper-silicon carbide composites using nanoindentation measurements. Ceramics International 2019; 45(7): 9164-9173.

Dash KB., Ray C., Chaira D. Synthesis and characterization of copper-alumina metal matrix composite by conventional and spark plasma sintering. Journal of Alloys and Compounds 2012; 516: 78–84.

Efe GC., Yener T., Altinsoy I., İpek M., Zeytin S., Bindal C. The effect of sintering temperature on some properties of Cu–SiC composite. Journal of Alloys and Compounds 2011; 509(20): 6036-6042.

Efe GC., İpek M., Zeytin S., Bindal C. An investigation of the effect of SiC particle size on Cu–SiC composites. Composites Part B: Engineering 2012; 43(4): 1813-1822.

Grzonka J., Kruszewski MJ., Rosiński M., Ciupiński Ł., Michalski A., Kurzydłowski, KJ. Interfacial microstructure of copper/diamond composites fabricated via a powder metallurgical route. Materials Characterization 2015; 99: 188-194.

Hu ZY., Zhang ZH., Cheng XW., Wang FC., Zhang YF., Li SL. A review of multi-physical fields induced phenomena and effects in spark plasma sintering: Fundamentals and applications. Materials and Design 2020; 191: 108662.

Kuskov KV., Abedi M., Moskovskikh DO., Serhiienko I., Mukasyan AS. Comparison of conventional and flash spark plasma sintering of Cu–Cr pseudo-alloys: Kinetics, structure, properties. Metals 2021; 11(1): 141.

Mallik AK., Reddy KM., Acikbas Calis N., Kara F., Mandal H., Basu D., Basu B. Influence of SiC addition on tribological properties of SiAlON. Ceramics International 2011; 37(7): 2495-2504.

Mallik AK., Acikbas Calis N., Kara F., Mandal H., Basu D. A comparative study of SiAlON ceramics. Ceramics International 2012; 38: 5757–5767.

Mallikarjuna HM., Ramesh CS., Koppad PG., Keshavamurthy R., Sethuram D. Nanoindentation and wear behaviour of copper based hybrid composites reinforced with SiC and MWCNTs synthesized by spark plasma sintering. Vacuum 2017; 145: 320-333.

Moustafa EB., Taha MA. Evaluation of the microstructure, thermal and mechanical properties of Cu/SiC nanocomposites fabricated by mechanical alloying. International Journal of Minerals, Metallurgy and Materials 2021; 28: 475-486.

Nair SV., Tien JK., Bates RC. SiC-reinforced aluminium metal matrix composites. International Materials Reviews 1985; 30: 275–290.

Nosewicz S., Romelczyk-Baishya B., Lumelskyj D., Chmielewski M., Bazarnik P., Jarząbek D., Pakieła Z. Experimental and numerical studies of micro-and macromechanical properties of modified copper–silicon carbide composites. International Journal of Solids and Structures 2019; 160: 187-200.

Pelleg J., Ruhr M., Ganor M. Control of the reaction at the fibre-matrix interface in a Cu/SiC metal matrix composite by modifying the matrix with 2.5 wt.% Fe. Materials Science and Engineering: A 1996; 212(1):139-148.

Schubert T., Brendel A., Schmid K., Koeck T., Zieliński W., Weißgärber T., Kieback B. Interfacial design of Cu/SiC composites prepared by powder metallurgy for heat sink applications. Composites part A: Applied science and Manufacturing 2007; 38(12): 2398-2403.

Shabani M., Paydar M. H., Zamiri R., Goodarzi M., Moshksar M. M. Microstructural and sliding wear behavior of SiC-particle reinforced copper matrix composites fabricated by sintering and sinter-forging processes. Journal of Materials Research and Technology 2016; 5(1): 5-12.

Shabani M., Paydar MH., Moshksar MM. Fabrication and densification enhancement of SiC-particulate-reinforced copper matrix composites prepared via the sinter-forging process. International Journal of Minerals, Metallurgy, and Materials 2014; 21: 934-939.

Shu KM., Tu GC. The microstructure and the thermal expansion characteristics of Cu/SiCp composites. Materials Science and Engineering: A 2003; 349(1-2): 236-247.

Shu S., Zhang Q., Ihde J., Yuan Q., Dai W., Wu M., Jiang N. Surface modification on copper particles toward graphene reinforced copper matrix composites for electrical engineering application. Journal of Alloys and Compounds 2022; 891: 162058.

Sundberg G., Paul P., Sung C., Vasilos T. Identification and characterization of diffusion barriers for Cu/SiC systems. Journal of Materials Science 2005; 40: 3383-3393.

Suryanarayanan K., Praveen R., Raghuraman S. Silicon carbide reinforced aluminium metal matrix composites for aerospace applications: A literature review. International Journal of Innovative Research in Science, Engineering and Technology 2013; 6336–6344.

Thankachan T., Prakash KS., Kavimani V. Investigating the effects of hybrid reinforcement particles on the microstructural, mechanical and tribological properties of friction stir processed copper surface composites. Composites Part B Engineering 2019; 174: 107057.

Tjong SC., Lau KC. Tribological behaviour of SiC particle-reinforced copper matrix composites. Materials Letters 2000; 43(5-6): 274-280.

Torabi H., Arghavanian R. Investigations on the corrosion resistance and microhardness of Cu–10 Sn/SiC composite manufactured by powder metallurgy process. Journal of Alloys and Compounds 2019; 806: 99-105.

Zhou W., Xu ZM. Casting of SiC reinforced metal matrix composites. Journal of Materials Processing Technology 1997; 63: 358–363.